IMPURITY IONS IN ASDEX UPGRADE AND WENDELSTEIN 7-AS STUDIED BY LITHIUM BEAM CHARGE-EXCHANGE SPECTROSCOPY

R. Brandenburg[1], S. Fiedler[2], J. Schweinzer[2], G. Petravich[3], F. Aumayr[1], HP. Winter[1], W7-AS and ASDEX Upgrade teams[2]

[1] *Institut für Allgemeine Physik, TU Wien, Association EURATOM-OEAW, A-1040 Wien, Austria*

[2] *Max-Planck-Institut für Plasmaphysik, EURATOM-Association, D-85748 Garching, Germany*

[3] *KFKI-Research Institute, Dept. of Plasma Physics, H-1525 Budapest, Hungary*

1. Introduction

Impurity ion concentration and -temperature in the core plasma region as well as the scrape-off layer are essential for understanding the physics of L- and H-mode transport and the transport barrier itself. To gain access to these properties, the well established Li-beam diagnostic capabilities on both fusion experiments at IPP Garching (ASDEX Upgrade tokamak and WENDELSTEIN 7 AS stellarator) have been extended [1] and now include the measurement of radial profiles of impurity-ion density and temperature by means of lithium beam charge-exchange spectroscopy (Li-CXS) [2,3,4,5].

2. Methodical principles

In competition with the impact excitation process, which serves for plasma electron density determination (Li-IXS), the weakly bound outer electron of the Li atom may also be captured by impurity ions. This charge-exchange process produces highly excited states of impurity ions and as a result characteristic impurity ion line radiation. Observation of such emitted spectral lines in conjunction with the modelled Li(*nl*) state distribution in the diagnostic beam allows for evaluation of the impurity density profile

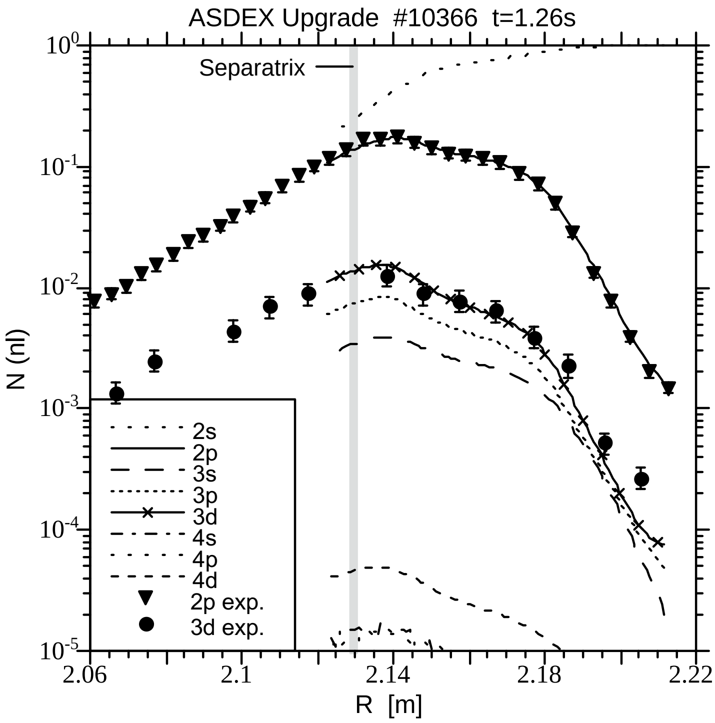

Fig. 1. Radial profiles of relative Li(*nl*) populations when the Li beam penetrates the plasma edge. Experimental results prove the reliability of the beam modelling.

along the beam. In addition, temperature profiles of impurity ions are derived from the respective spectral line shapes. Determination of absolute values from the diagnostic raw data requires a reliable database as well as a detailed modelling [6] of the diagnostic beam which has been checked recently [7] by observing the Li(*3d*→*2p*) spectral line. Taking into account that the Li(*3d*) level represents less than 1% of the beam atoms, excellent agreement between experimental results and theoretical values demonstrate a now satisfactory status of the beam modeling (Fig. 1). Effective emission cross sections which describe charge exchange processes between Li atoms and impurity ions are calculated within the ADAS file system [8].

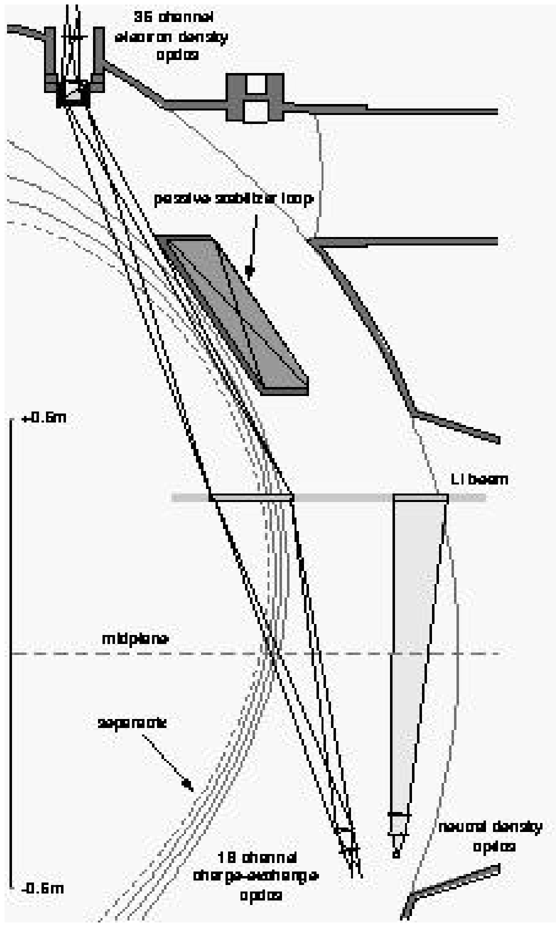

Fig. 2. Optical observation systems of extended lithium beam diagnostics on ASDEX Upgrade.

Evaluation of impurity density profiles

The current setups on both experiments have already been described extensively [1,9]. To determine the absolute concentration of impurity ions, both Li beam diagnostic methods are applied simultaneously [9]. While the photomultipliers of the IXS system record the Li(*2p*→*2s*) light emission at λ = 670.8 nm, the CXS system (spectrometer + CCD camera) detects the impurity ion radiation. Since both systems use different observation optics (cf. Fig. 2), the detection efficiency has to be cross-calibrated. This is done by measuring the Li(*2p*→*2s*) radiation with both systems in one calibration discharge, as described in Eqs. (1a/b).

$$U_{2p}^{IXS}(i) = k_{671}^{IXS}(i) \cdot n_{Li} \cdot A_{2p\rightarrow 2s} \cdot N(2p)$$
$$U_{2p}^{CCD}(i) = k_{671}^{CCD}(i) \cdot n_{Li} \cdot A_{2p\rightarrow 2s} \cdot N(2p) \qquad \text{(1a/b)}$$

k denotes the detection efficiency for the two systems at λ = 671.0 nm, i the corresponding radial channel, $A_{2p\rightarrow 2s}$ the transition probability, n_{Li} the particle density of the Li-beam and *N(2p)* the relative occupation number of the Li(*2p*)-state. The CXS-signal ($U_{imp}^{CCD}(i)$) can be expressed by

$$U_{imp}^{CCD}(i) = k_{imp}^{CCD}(i) \cdot v_{Li} \cdot n_{imp} \cdot n_{Li} \cdot \sum_{nl} \sigma_{em}(nl) \cdot N(nl) \qquad (2)$$

Calculating the ratio of Eqs. (1b) and (2) for the discharges in question and using the ratio of Eqs. (1a) and (1b) for the calibration discharge, the impurity ion density can be expressed by

$$n_{imp}(z_{Li}(i)) = \frac{U^{CCD}_{imp}(i)}{U^{IXS}_{2p}(i)} \cdot \frac{k^{IXS}_{671}(i)}{k^{CCD}_{671}(i)} \cdot \frac{k^{CCD}_{671}(i)}{k^{CCD}_{imp}(i)} \cdot \frac{A_{2p\to 2s} \cdot N(2p)}{v_{Li} \cdot \sum_{nl} \sigma_{em}(nl) \cdot N(nl)} \qquad (3)$$

for different radial positions z_{Li} along the beam line. In Eq. (3), the first ratio relates the measured signals of both systems, the second ratio is determined by the calibration procedure (see above) and the third ratio expresses the different detection probabilities of the CCD camera at the two wavelengths. v_{Li} denotes the Li-beam particle velocity and $\sigma_{em}(nl)$ the cross section for emission following electron capture from the Li(*nl*)-level. The relative occupation numbers *N(nl)* of the Li-beam atoms are calculated in the reconstruction process for the electron density [6].

With the current setups, spatial resolution is $\Delta x = 0.5$ cm on W7AS and 1 cm on ASDEX Upgrade; temporal resolution is limited by the readout time of the CCD camera to 80 ms for 16 simultaneous measurements.

3. Results

CXS investigations on W7-AS

The described algorithm was applied in a series of equivalent discharges (P_{ECRH} = 400kW, D_2, $\iota = 0.34$, B_z = 20.0 mT, up/down limiters attached, $\int \nu_\varepsilon \delta\lambda$(HCN) = $2 \cdot 10^{19}$ m^{-2}) to determine the C^{6+} density at different radial positions. As shown in Fig. 3, the C^{6+} concentration increases from about 0.41% at r_{eff} = 16.7 cm to 0.63% at r_{eff} = 8.3 cm. In the gradient region of the profile good agreement is found with results from hydrogen beam CXS diagnostics [10].

Simulation of charge state distribution

The IONEQ code [11] was used to simulate the radial charge state distribution of carbon in W7-AS plasmas. Within this simulation the carbon ion distribution is calculated according to the Corona equilibrium. In addition the neoclassical impurity transport fluxes are modeled by assuming reasonable values for a diffusion coefficient and a convection velocity. As input data the electron density profile from the Li beam and the temperature profile from the Thomson diagnostics was used. The neutral gas density was modeled by the EIRENE code and calibrated with the H_α as well as the neutral density measurement of the Li beam

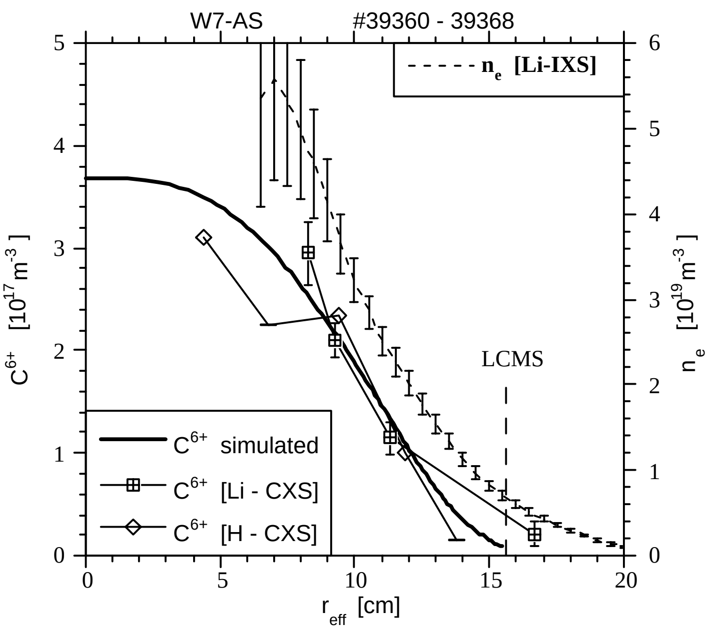

Fig. 3. Radial C^{6+} and electron density profiles as a function of effective radius r_{eff} for discharges #39360 - 39368. The strong line shows the result of a simulation with the IONEQ code.

diagnostics [12]. Good agreement was achieved with a strong inwards velocity of $v=-4D/r_{LCFS}$ (diffusion coefficient D = 0.2 m^2s^{-1}) [13].

CXS investigations on ASDEX Upgrade

On ASDEX Upgrade we use the spectrometer and CCD camera for investigation of impurity ion spectral lines in the range from 250 < λ < 800 nm. Although the complex temporal behaviour of the ASDEX Upgrade discharges poses severe difficulties for the Li-CXS method with the current setup, first results indicate the feasibility of Li-CXS for several impurities (He^+, B^{2+}, O^+, F^+, Ne^{6+}, Ne^{10+}). Comparing radial resolution of data obtained with the Li beam and the hydrogen heating beam, respectively, we can clearly demonstrate the advantage of the Li-CXS method in the plasma edge (Fig. 4).

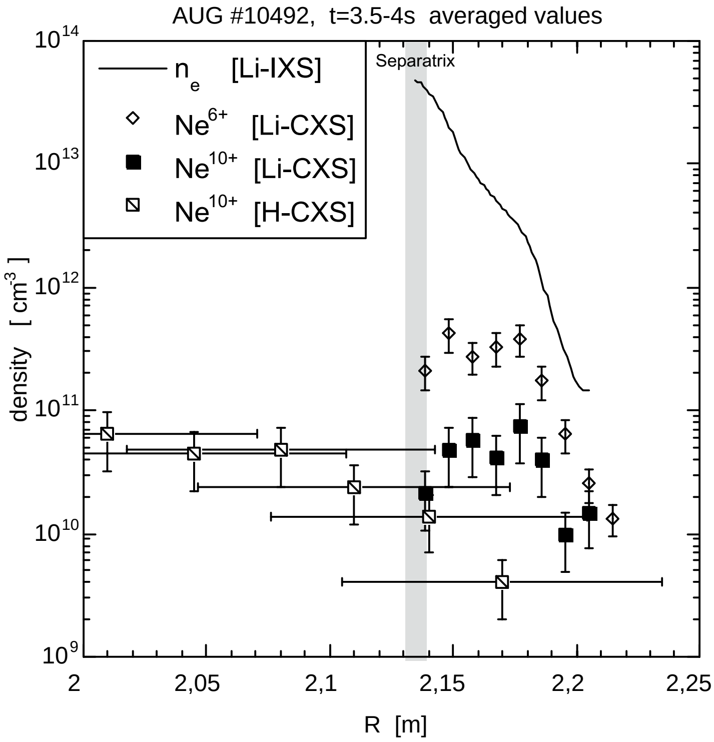

Fig. 4. Radial profiles of Ne^{6+}, Ne^{10+} and electron densities in a discharge with a strong Ne gas puff. Spatial resolution is much higher for Li-CXS than for H-CXS. Signals have been averaged in order to reduce scatter. Ne^{6+} data contain undetermined contributions from C^{6+} (both at λ = 529 nm) and appear systematically too high.

Acknowledgments

This work has been supported by Friedrich Schiedel-Stiftung für Energietechnik and by Kommission zur Koordination der Kernfusionsforschung at the Austrian Academy of Sciences.

References

[1] R. Brandenburg et al.: *24th EPS Conf.*, Europhys.Conf.Abstr. **21A** Part I (1997) 477
[2] E. Wolfrum et al.: Rev. Sci. Instrum. **64** (1993) 2285
[3] F. Aumayr et al.: J. Nucl. Materials **196-198** (1992) 928
[4] R.P. Schorn et al.: Nucl. Fusion **32** (1992) 351
[5] HP. Winter: Comments At. Mol. Phys. **12** (1982) 165
[6] J. Schweinzer et al.: Plasma Phys. Contr. Fusion **34** (1992) 1173
[7] R. Brandenburg et al.: *to be published*
[8] http://patiala.phys.strath.ac.uk/adas/adas.html
[9] S. Fiedler et al.: *13. PSI Conf.*, San Diego (1998), *to be published in* J. Nucl. Mat.
[10] J. Baldzuhn et al.: Rev. Sci. Instrum. **68** (1997) 1020
[11] A. Weller, D. Pasini, A.W. Edwards, R.D. Gill and R. Granetz: JET-IR (87) 10
[12] S. Fiedler et al.: *23rd EPS Conf.*, Europhys.Conf.Abstr. **20C** Part III (1996) 1009
[13] S. Fiedler et al.: J. Plasma and Fusion Res. SERIES, Vol. 1 (1998)